CATARACT

Comparison of anterior segment and lens biometric measurements in patients with cataract

Shinichi Fukuda[1] · Yuta Ueno[1] · Akari Fujita[1] · Haruhiro Mori[1] · Kuniharu Tasaki[1] · Tomoya Murakami[1] · Simone Beheregaray[2] · Tetsuro Oshika[1]

Abstract

Purpose This study was performed to compare anterior ocular biometric measurements of deep-range swept-source anterior segment optical coherence tomography (AS-OCT) (CASIA2) versus short-range swept-source AS-OCT (CASIA SS-1000), ultrasonography (AL-4000), and Scheimpflug camera analysis (Pentacam and EAS-1000) in patients with cataract.
Methods One hundred eighty-five eyes of 128 participants with mild refractive error or cataract were examined. The central corneal thickness (CCT), aqueous depth (AQD), and lens thickness were obtained. The repeatability of CASIA2 measurements was assessed.
Results In patients with cataract, the CCT, AQD, lens thickness, and lens anterior curvature by CASIA2 showed high intraclass correlation coefficients (ICCs) of > 0.99. Conversely, measurements of the posterior part of the lens such as lens posterior curvature showed lower ICCs. The ICCs were higher in healthy young participants than in patients with cataract. The ICCs tended to be lower in patients with mild than dense cataract. There was no statistically significant difference in the CCT and AQD between the CASIA2 and CASIA SS-1000 or in the lens thickness measurements between the CASIA2 and AL-4000 and between the CASIA2 and EAS-1000. There was a significant linear correlation in the biometric measurements between the CASIA2 and the other instruments.
Conclusion We evaluated the biometric measurements of the anterior eye segment by the CASIA2. The CASIA2 yielded results comparable with those of the CASIA SS-1000, ultrasonography, and Scheimpflug camera. However, mild cataract decreased the repeatability of measurements of the posterior part of the lens.

Keywords Deep-range swept-source anterior segment optical coherence tomography · CASIA2 · Lens biometry · Anterior segment biometry · Cataract

Introduction

Accurate and precise ocular biometry is crucial for the diagnosis and treatment of ocular disorders. Several noninvasive or marginally invasive techniques have been used for anterior ocular biometric measurements, including crystalline lens shape evaluation, slit-lamp photography [1, 2], A-scan ultrasonography [3], examination with a Scheimpflug camera [4], and optical coherence tomography (OCT) [5, 6]. Measurement of the central corneal thickness (CCT) is useful to reduce the risk of postoperative ectasia when screening for refractive surgery and is crucial in the evaluation of contact lens-induced edema [7], measurement of the intraocular pressure [8], and diagnosis of corneal diseases such as keratoconus [9]. Measurement of the anterior chamber depth (ACD) is important when screening for primary angle closure glaucoma [10], monitoring the changes of the anterior segment during accommodation [11], and calculating phakic intraocular lenses [12]. The lens thickness is important for biometric studies of lens development as it relates to aging, myopia, presbyopia, accommodation, and primary angle-closure glaucoma [13–16].

SF and UY contributed equally to this work

✉ Shinichi Fukuda
caesar.shihtzu@gmail.com

[1] Department of Ophthalmology, Faculty of Medicine, University of Tsukuba, 1-1-1 Tennoudai, Tsukuba, Ibaraki 305-8575, Japan

[2] Department of Ophthalmology, The Queen Elizabeth Hospital, Adelaide, South Australia, Australia

OCT is a noninvasive imaging technique that uses low-coherence light to obtain a high-resolution cross-section of biological structures [17]. The first-generation anterior segment OCT (AS-OCT) system with 1310-nm wavelength light was based on a time-domain OCT method that depends on a moving reference mirror to scan each depth position in the image pixel [18, 19]. The CASIA SS-1000 (Tomey, Nagoya, Japan), a second-generation AS-OCT system based on swept-source OCT technology, which is a variation of Fourier domain analysis, can obtain images 10 times faster than time-domain OCT [20]. The CASIA SS-1000 measures tissue with a maximum width of 16 × 16 mm and a maximum depth of 6 mm. It achieves high-resolution imaging (10 μm axially and 30 μm transversally) and high-speed scanning of 30,000 A-scans per second and is capable of obtaining full three-dimensional images of ocular tissues. The CASIA2 (Tomey) is a further development of the CASIA SS-1000 and is capable of reaching a scan speed of 50,000 A-scans per second [21]. One of the main differences between the two devices is the range of measurement depth. The CASIA2 measures tissue with a maximum depth of 13.0 mm, which is more than twice the value recorded by the CASIA SS-1000.

The CASIA2 allows the user to obtain a whole image from the cornea to the posterior lens. No previous studies have compared the CASIA2 with the CASIA SS-1000 or other standard anterior segment measurement instrument, such as A-scan ultrasonography or the Scheimpflug camera, for central corneal thickness (CCT)/aqueous depth (AQD)/lens thickness measurements in patients with cataract. Therefore, we conducted the current study to compare the results of biometric measurements performed by the CASIA2, CASIA SS-1000, A-scan ultrasonography (AL-4000; Tomey), and Scheimpflug cameras (Pentacam is a rotating Scheimpflug camera and was introduced in 2002; Oculus, Wetzlar, Germany. EAS-1000 was the first commercially available Scheimpflug slit imaging instrument at the end of the 1980s; Nidek Co. Ltd., Tokyo, Japan). We also evaluated anterior ocular biometric parameters including the crystalline lens and assessed their repeatability in healthy young participants and patients with cataract.

Patients and methods

We conducted an investigation in a Tsukuba University Hospital. This study followed the tenets of the Declaration of Helsinki, and written informed consent was obtained from each participant. The institutional review board of Tsukuba University Hospital approved the study. Two experienced examiners (A.F. and Y.U.) sequentially performed the measurements using AS-OCT (CASIA2 and CASIA SS-1000), a rotating Scheimpflug camera (Pentacam), ultrasonic pachymetry (AL-4000), and a Scheimpflug camera (EAS-1000). The CASIA

SS-1000 is a Fourier-domain, swept-source OCT system designed specifically for imaging the anterior segment. The CASIA SS-1000 achieves high-resolution imaging (10 μm axially and 30 μm transversally) and high-speed scanning of 30,000 A-scans per second. The wide scanning range of 16 mm allows observation of the area from the whole angle at once. The depth scan range is 6 mm (in air). The CASIA2 is anterior segment swept-source OCT system with a scan speed of 50,000 A-scans per second. The depth scan range was improved to 13 mm (in air). The EAS-1000 is the first commercially available Scheimpflug slit imaging instrument. The Pentacam is a rotating Scheimpflug camera. The Pentacam includes software to analyze the different captured meridians on cross-sectional images and transform them into a three-dimensional model for related quantitative measurements, which can take up to 2 s. The AL-4000 is a handheld ultrasound biometer that communicates with the OA-2000 via Bluetooth technology. The participants were instructed to look at an internal fixation target during the scanning. All measurements were recorded between 11:00 a.m. and 3:00 p.m. The examination room was illuminated at 6.0 ± 1.5 lux as measured with a light meter (LM-8000; Fuso, Tokyo, Japan). Cataract classification and grading were performed using the Lens Opacities Classification System III. The exclusion criteria were previous ocular surgery, trauma, active ocular disease, fundus disease, and poor fixation.

On the OCT images, a line was placed from angle to angle with a perpendicular projection that extends from a median point forward through the cornea. Along this perpendicular line, the CCT, AQD, and ACD were measured. The CCT was defined as a distance from anterior to posterior cornea (Fig. 1a white line), AQD was defined as the distance of the posterior face of the cornea to the anterior surface of the lens (Fig. 1a blue line). The lens thickness was defined as a distance from anterior to posterior lens on vertex normal (Fig. 1a orange line) [22]. The anterior chamber depth (ACD) was defined as the distance from the central corneal epithelium to the anterior surface of the lens and same as adding value CCT and AQD (CCT + AQD). Equator of lens was defined as a point of intersection of lines that is extension of anterior and posterior surface of lens. Equator diameter was diameter of the center of equator circle of lens (Fig. 1a yellow line). Optic axis was defined as a perpendicular line with the center of equator circle of lens. The amount of decentration was defined as a distance between vertex normal and the center of equator circle of lens. Tilting amount was defined as an angle between vertex normal and optic axis. Lens equatorial plane (without CCT) was a distance between posterior of the cornea and a center of equator circle of lens on optic axis (Fig. 1a red line) [23]. The built-in software in the CASIA2 automatically drew the anterior and posterior lens boundaries and calculated the lens thickness, anterior and posterior lens curvature, amount of decentration, tilting amount, equator diameter, and lens equatorial plane (without CCT) on the visual axis (Fig. 1a).
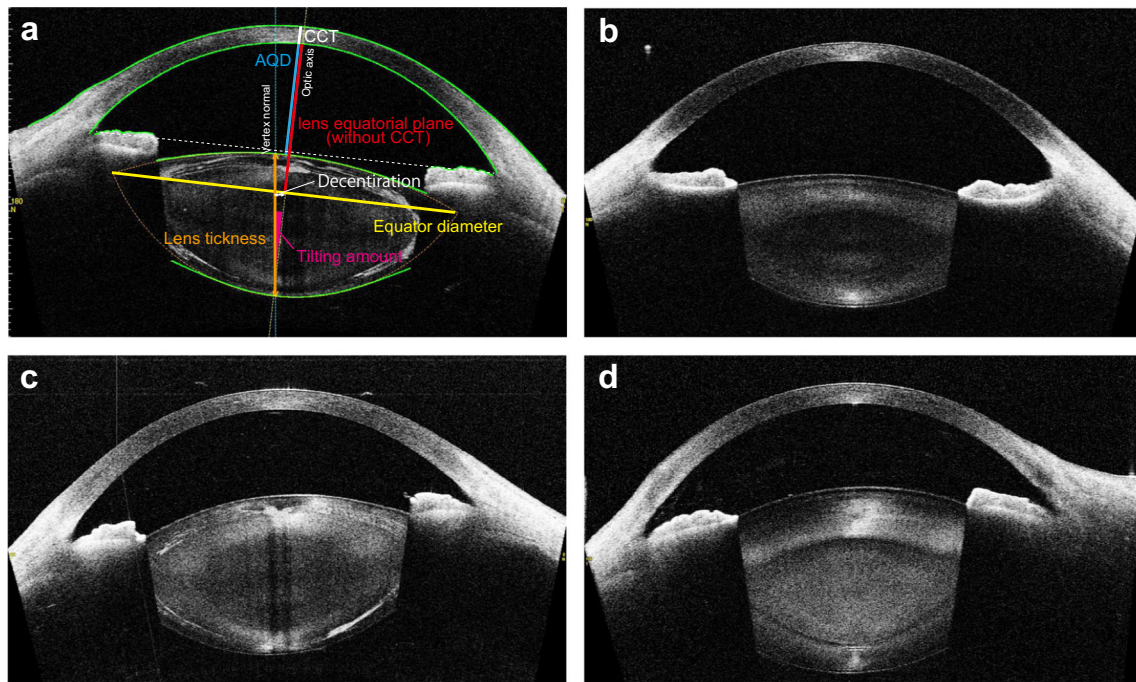
Fig. 1 Representative images of the CASIA2. The built-in software in the CASIA2 automatically draws the anterior and posterior lens boundaries and calculates the lens thickness, anterior and posterior lens curvature, amount of decentration, tilting amount, equator diameter, and lens equatorial plane (without CCT) (**a**). A 30-year-old normal participant (**b**). A 69-year-old man with grade 4 cortical cataract (**c**). A 67-year-old woman with grade 3 nuclear cataract (**d**)

The CCT and AQD (from the endothelium to the surface of lens) obtained by the CASIA2 and CASIA SS-1000, the lens thickness and ACD (CCT + AQD) obtained by the CASIA2 and AL-4000, the AQD obtained by the CASIA2 and Pentacam, and the lens thickness and AQD obtained by the CASIA2 and EAS-1000 were compared using the Wilcoxon signed-rank test and Bland–Altman plots [24]. The 95% limits of agreement (mean difference ± 1.96 standard deviation), which define the range that encompasses most differences between the measurements by two methods, was calculated. Pearson's correlation coefficient between each method was also evaluated.

Table 1 Anterior ocular biometry measurements by CASIA 2

	Cataract patients		Young control	
	$n = 135$		$n = 50$	
Age	72.1 ± 8.1		30.1 ± 3.9	
LOCSIII grading				
Nuclear opalescence or color	2.5 ± 0.7		1.0 ± 0.0	
Cortical cataract	1.9 ± 1.1		1.0 ± 0.0	
Posterior subcapsular cataract	1.3 ± 0.8		1.0 ± 0.0	
	Mean ± SD	ICC	Mean ± SD	ICC
CCT	526.07 ± 41.04 μm	0.996	531.43 ± 30.81 μm	0.994
AQD	2.72 ± 0.36 mm	0.998	3.29 ± 0.27 mm	0.998
Lens thickness	4.56 ± 0.39 mm	0.995	3.77 ± 0.20 mm	0.998
Lens anterior curvature	9.66 ± 1.41 mm	0.993	12.16 ± 1.60 mm	0.996
Lens posterior curvature	5.81 ± 0.56 mm	0.674	6.09 ± 0.40 mm	0.937
Amount of decentration	0.17 ± 0.10 mm	0.536	0.19 ± 0.07 mm	0.954
Tilting amount	4.86 ± 1.52 °	0.836	4.23 ± 1.43 °	0.961
Equator diameter	10.14 ± 0.61 mm	0.827	10.03 ± 0.32 mm	0.924
Equatorial lens depth (without CCT)	4.21 ± 0.27 mm	0.881	4.39 ± 0.25 mm	0.991

Values are presented as mean ± standard deviation

CCT central corneal thickness, *AQD* aqueous depth, *ICC* Intraclass correlation coefficient

To evaluate repeatability, the intraclass correlation coefficients (ICCs) of the anterior biometric parameters (CCT, AQD, lens thickness, anterior and posterior lens curvature, amount of decentration, tilting amount, equator diameter, and lens equatorial plane (without CCT)) obtained by the CASIA2 were evaluated. The correlation between the amount of differences in two measurements and cataract density was assessed using Spearman's rank correlation coefficient.

All tests of association were considered statistically significant at $P < 0.05$. Analyses were carried out using StatView (SAS Institute, Cary, NC).

Results

We examined 185 eyes of 128 participants (58 men and 70 women) without ocular abnormalities other than mild refractive error or cataract. The participants' age (mean ± standard deviation) was 60.5 ± 20.1 years (range, 26–90 years). The refractive mean spherical equivalent error was 0.66 ± 1.36 D (range 2.88 to 2.38 D).

Biometric measurements in patients with cataract and young normal participants using the CASIA2

Representative images obtained by the CASIA2 are shown in Fig. 1. The images were obtained from a 30-year-old man in the normal participant group (Fig. 1b), a 69-year-old woman with grade 4 cortical cataract (Fig. 1c), and a 67-year-old man with grade 3 nuclear cataract (Fig. 1d). We examined 135 eyes of 78 patients with cataract (32 men and 46 women) aged 72.1 ± 8.1 years (range, 56–90 years). The refractive mean spherical equivalent error was 0.39 ± 1.21 D (range 2.88 to 2.38 D). The mean CCT, AQD, lens thickness, anterior lens curvature, and posterior lens curvature with the CASIA2 were 526.07 ± 41.04 μm, 2.72 ± 0.36 mm, 4.56 ± 0.39 mm, 9.66 ± 1.41 mm, and 5.81 ± 0.56 mm, respectively ($n = 135$). We also measured the details of lens morphology, such as the amount of decentration, tilting, equator diameter, and lens equatorial plane (without CCT) (Table 1). In the repeatability analysis of the CASIA2, the anterior parameters (CCT, AQD, lens thickness, and anterior lens curvature) showed high ICCs of > 0.99. Conversely, the posterior parameters involving the back side of the lens (posterior lens curvature, amount of decentration, tilting amount, equator diameter, and lens equatorial plane (without CCT)) showed low ICCs (Table 1). To investigate whether the low ICCs were due to the presence of cataract, we assessed the measurement repeatability in the healthy young participants (50 eyes of 50 participants; age, 30.1 ± 3.9 years; range, 26–39 years, the refractive mean spherical equivalent error; − 1.36 ± 1.47 D (range, − 2.75 to 0.5 D).). The healthy young participants showed higher ICCs

Table 2 Density and type of cataract and repeatability of CASIA2 measurements

Nuclear opalescence or color	Cortical cataract	Posterior subcapsular cataract	n	AQD (ICCs)	Lens thickness	Anterior curvature	Posterior Curvature	Amount of decentration	Tilting amount	Equator diameter	Lens equatorial plane (without CCT)
Grade 2	Grade 1	Grade 1	32	1.000	0.988	0.983	0.378	0.383	0.828	0.558	0.747
Grade 3	Grade 1	Grade 1	17	0.999	0.995	0.996	0.694	0.865	0.963	0.761	0.912
Grade 4 or 5	Grade 1	Grade 1	3	0.999	1.000	0.995	0.984	0.998	0.962	0.996	0.991
Grade 2	Grade 1	Grade 1	32	1.000	0.988	0.983	0.378	0.383	0.828	0.558	0.747
Grade 2	Grade 2	Grade 1	20	0.999	0.988	0.985	0.979	0.842	0.951	0.928	0.964
Grade 2	Grade 3	Grade 1	16	0.999	0.997	0.997	0.771	0.350	0.874	0.823	0.985
Grade 2	Grade 4	Grade 1	6	1.000	0.999	0.994	0.911	0.899	0.634	0.988	0.980
Grade 2	Grade 1	Grade 1	32	1.000	0.988	0.983	0.378	0.383	0.828	0.558	0.747
Grade 2	Grade 1	Grade 3 or 4	4	1.000	0.993	0.995	0.674	0.191	0.929	0.940	0.901

AQD aqueous depth, *ICCs* Intraclass correlation coefficients

than the aged patients with cataract. All ICCs were > 0.9 (Table 1).

Density and type of cataract and repeatability of CASIA2 measurements

To evaluate whether the density or type of cataract affected the ICCs of the CASIA2, we calculated the ICCs in each nuclear, cortical, and posterior subcapsular cataract subtype. Same as uncategorized total 135 eyes with cataract, the anterior parameters such as the AQD, lens thickness, and anterior lens curvature of each cataract subtype showed a high ICC. Conversely, the posterior parameters involving the back side of the lens such as the posterior lens curvature, amount of decentration, tilting amount, equator diameter, and lens equatorial plane (without CCT) showed low ICCs in each group (Table 2). The amount of differences between the first and second measurement was not correlated with the density of cataract in each cataract subtype ($P > 0.05$, Spearman's rank correlation coefficient). Interestingly, the ICCs tended to show better values in patients with dense cataract (Table 2). Mild nuclear cataract (nuclear opalescence or color grade 2, cortical grade 1, posterior subcapsular grade 1 group) showed the worst ICCs among the posterior lens parameter measurements

(lens posterior curvature, amount of decentration, tilting amount, equator diameter, and lens equatorial plane (without CCT)).

CASIA2 measurements compared with CASIA SS-1000, AL-4000, Pentacam, and EAS-1000 measurements

The mean CCT and AQD with the CASIA SS-1000 were 527.1 ± 39.4 μm and 2.77 ± 0.40 mm, respectively ($n = 65$). The mean ACD (CCT + AQD) and lens thickness with the AL-4000 were 3.20 ± 0.34 mm and 4.59 ± 0.39 mm, respectively ($n = 74$). The mean AQD with the Pentacam was 2.66 ± 0.34 mm ($n = 66$). The mean lens thickness and AQD were measured by EAS-1000, and it were 4.36 ± 0.43 mm ($n = 19$) and 2.71 ± 0.38 mm ($n = 71$), respectively. There was no statistically significant difference in the CCT or AQD measurements between the CASIA2 and CASIA SS-1000 (527.8 ± 39.4 μm and 2.78 ± 0.36 mm for CASIA2, 527.1 ± 39.4 μm and 2.77 ± 0.40 mm for CASIA SS-1000, $P = 0.991$ and $P = 0.864$, respectively; Wilcoxon signed-rank test), in the lens thickness measurements between the CASIA2 and EAS-1000 (4.37 ± 0.41 mm for CASIA2, 4.36 ± 0.43 mm for EAS-1000, $P = 0.586$, Wilcoxon signed-rank test), or in the lens thickness measurements between the CASIA2 and AL-
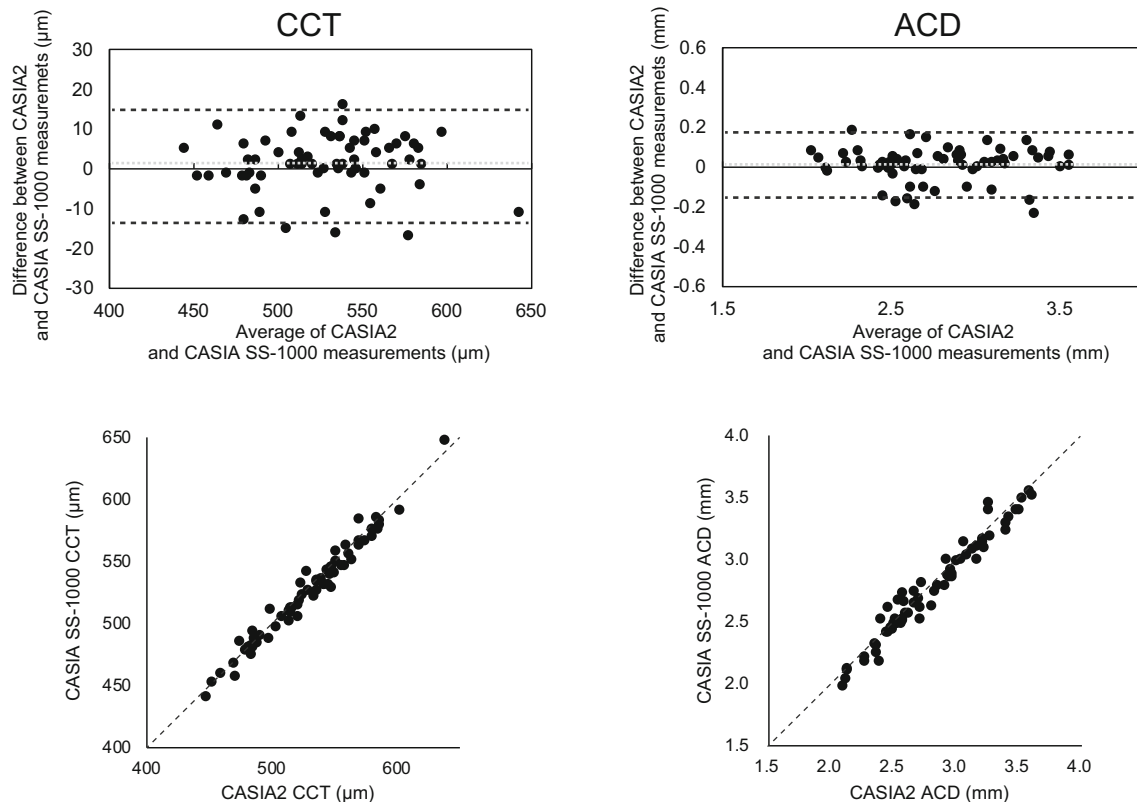
Fig. 2 A significant correlation in the central corneal thickness (CCT) and aqueous depth (AQD) was observed between the CASIA2 and CASIA SS-1000 (Pearson correlation coefficient, r = 0.334, P < 0.0001 and r = 0.694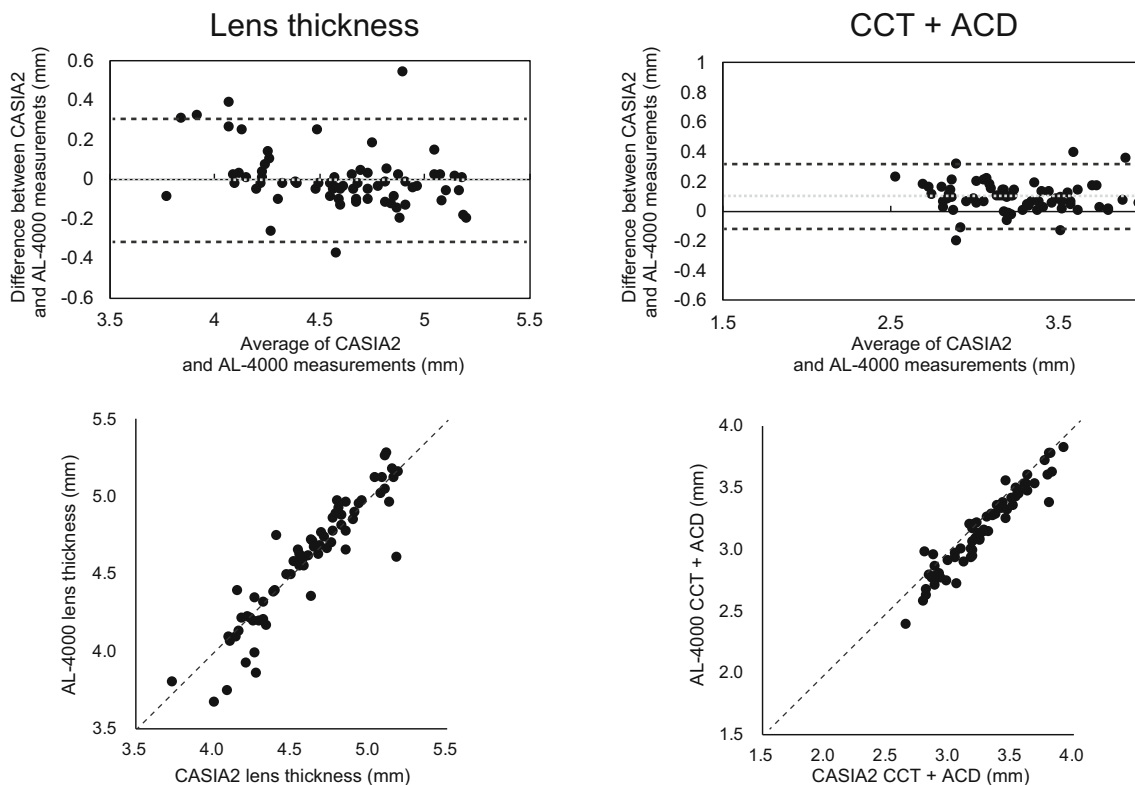, P < 0.0001, respectively). The line of equivalence (y = x) is shown by the dotted line. The difference in the mean CCT measurements between the CASIA2 and CASIA SS-1000 is shown. The mean ± 1.96 standard deviation is also indicated

4000 (4.59 ± 0.36 mm for CASIA2, 4.59 ± 0.39 mm for AL-4000, P = 0.171, Wilcoxon signed-rank test). Conversely, there was a significant difference in the ACD (CCT + AQD) measurements between the CASIA2 and AL-4000 (2.97 ± 0.34 mm for CASIA2, 3.20 ± 0.34 mm for AL-4000. P < 0.001, Wilcoxon signed-rank test), in the AQD measurements between the CASIA2 and Pentacam (2.76 ± 0.31 for CASIA2, 2.66 ± 0.34 for Pentacam, P < 0.0001, Wilcoxon signed-rank test), and in the AQD measurements between the CASIA2 and EAS-1000 (2.74 ± 0.39 for CASIA2, 2.71 ± 0.38 for EAS-1000, P < 0.0001, Wilcoxon signed-rank test). There was a significant linear correlation of the biometric measurements between the CASIA2 and the other instruments (P < 0.0001) (Figs. 2, 3, 4, and 5). Bland–Altman plots to assess the difference are shown in Figs. 2, 3, 4, and 5. The mean differences in the CCT and AQD measurements were 1.38 ± 7.03 μm and 0.01 ± 0.09 mm, respectively, between the CASIA2 and CASIA SS-1000. The mean differences in the ACD (CCT + AQD) and lens thickness measurements were − 0.44 ± 0.14 mm and 0.00 ± 0.15 mm, respectively, between the CASIA2 and AL-4000. The mean difference in the AQD measurement was 0.10 ± 0.07 mm between the CASIA2 and Pentacam. Finally, the mean differences in the lens thickness and AQD measurements were 0.02 ± 0.25 mm and 0.04 ±

0.09 mm, respectively, between the CASIA2 and EAS-1000. The posterior lens could be imaged by the Pentacam in only 6% of patients and by the EAS-1000 in 27% of patients.

Discussion

This study compared the CASIA2 with the CASIA SS-1000, A-scan ultrasonography, and Scheimpflug cameras. To the best of our knowledge, this is the first study to compare the CASIA SS-1000 and deep-range anterior segment swept-source OCT CASIA2 in patients with cataract. Moreover, no previous lens biometry studies have assessed the repeatability of measurements using the CASIA2 in patients with cataract and healthy young subjects. The imaging depth of the CASIA SS-1000 was not sufficient to image the whole anterior segment including the cornea and crystalline lens, which requires an axial range of approximately 12.0 mm. To overcome this limitation, the authors of a previous study moved the position of the OCT scan head closer to the patient's eye [25]. Lens imaging by the CASIA SS-1000 is limited in that the internal structures of the crystalline lens cannot be clearly distinguished and measured due to overlap of the real and mirror images of the lens [25]. Another limitation of lens imaging by

Fig. 3 Significant correlations in the lens thickness and central corneal thickness + anterior chamber depth ACD (central corneal thickness (CCT) + aqueous depth (AQD)) were observed between the CASIA2 and AL-4000 (Pearson correlation coefficient, r = 0.926, P < 0.0001

and r = 0.956, P < 0.0001, respectively). The line of equivalence ($y = x$) is shown by the dotted line. The difference in mean CCT measurements between the CASIA2 and AL-4000 is shown. The mean ± 1.96 standard deviation is also indicated

ACD
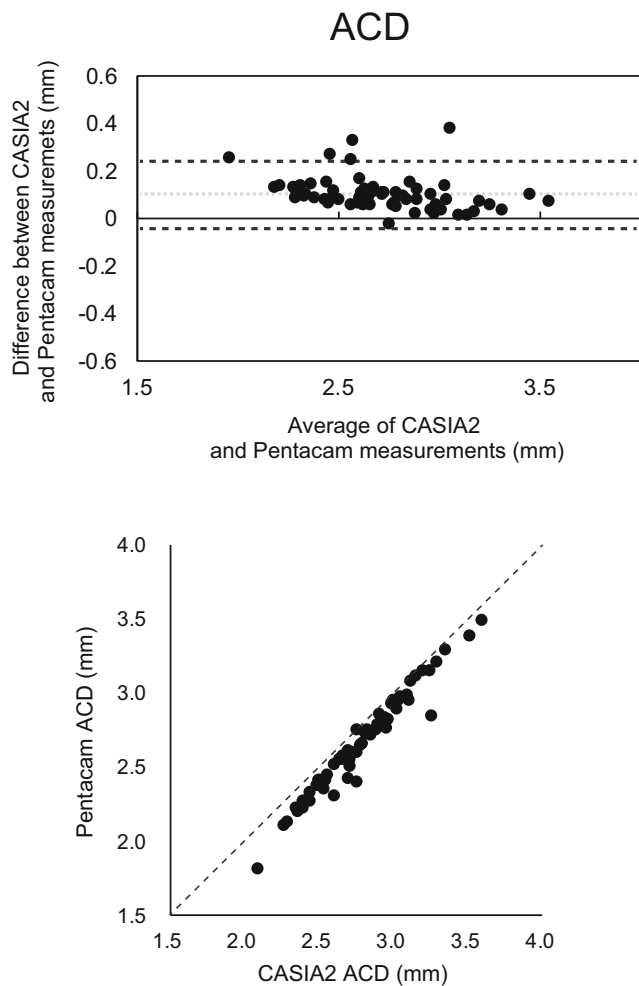
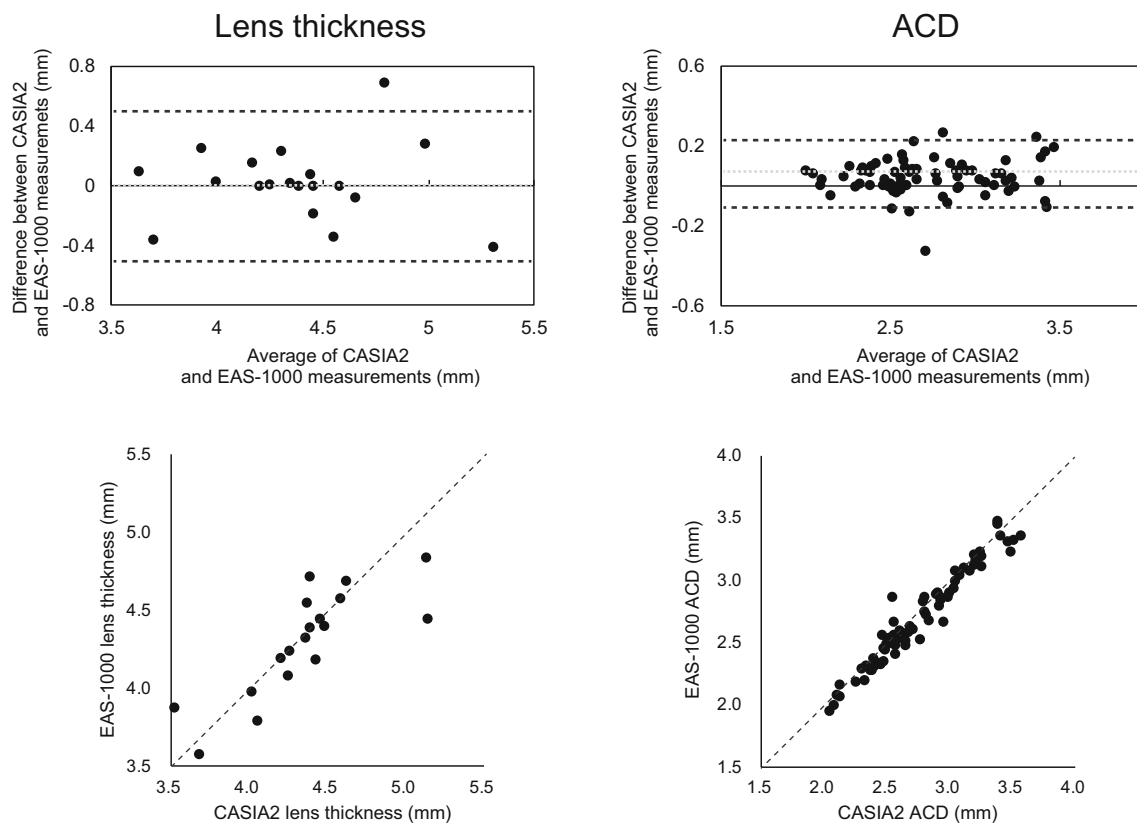

Fig. 4 A significant correlation in the aqueous depth (AQD) was observed between the CASIA2 and Pentacam (Pearson correlation coefficient, r = 0.980, P < 0.0001). The line of equivalence (y = x) is shown by the dotted line. The difference in the mean aqueous depth (AQD) measurements between the CASIA2 and Pentacam is shown. The mean ± 1.96 standard deviation is also indicated

the commercially available CASIA SS-1000 is that the posterior part of the crystalline lens is vertically inverted; thus, the software provided with the clinical system cannot be used to correct for distortion of the images caused by refraction. Several reports have evaluated anterior segment biometry, including the whole crystalline lens, in a single image using custom-made OCT devices [5, 26, 27]. However, these custom-made OCT devices were laboratory-based and have limited clinical use. In contrast, the CASIA2 is commercially available and has various built-in programs that enable automatic calculation of anterior segment biometry, including the whole crystalline lens. Xu et al. reported good reproducibility of the measurement of anterior segment parameters such as lens vault, pupil diameter, anterior chamber width, angle opening distance, trabecular iris space area, and scleral spur angle between the CASIA2 and Spectralis OCT2 (Heidelberg Engineering, Heidelberg, Germany) [28]. Chansangpetch

et al. measured the angle opening distance, trabecular iris space area, angle recess area, ACD, anterior chamber width, and lens vault by the CASIA2 and time-domain AS-OCT. They reported that both devices had generally good agreement. However, there were proportional and constant biases in most angle parameters [29]. Shoji et al. reported good reproducibility of in vivo crystalline lens measurements for healthy young subjects obtained by the CASIA2. The authors reported that the intraobserver and intervisit ICCs for lens thickness measurement varied from 0.980 to 0.992 and from 0.942 to 0.995, respectively [21]. The current study showed similar results. In the current study, the anterior parameters such as CCT, AQD, lens thickness, and anterior lens curvature showed high ICCs (> 0.993). Conversely, the posterior parameters involving the back side of the lens, such as the amount of decentration, tilting, equator diameter, and lens equatorial plane (without CCT), showed low ICCs in patients with cataract. In the present study, the healthy young participants showed higher ICCs than the aged patients with cataract. One reason for these findings is that the signal strength in OCT generally decreases with deeper penetration in the axial direction. Interestingly, the ICCs tended to be better in patients with dense than mild cataract (Table 2). The delineation of the posterior surface of the lens tended to be clearer in patients with densethan mild cataract. This might be the reason why mild cataract showed the worst ICCs in the posterior lens parameter measurements. In the OCT system, distortion was corrected using refractive indices of the lens and aqueous. In the current study, the lens refractive index was set at 1.4085. This value may not be correct because there is often a gradient of refractive indices across the thickness of the crystalline lens. Cataracts may also affect the refractive indices of the lens. The heterogeneity of the lens refractive index in patients with mild cataract may cause low repeatability. Interestingly, a previous study showed that the posterior lens curvature tended to have better reproducibility than anterior curvature measurements [21]. The mean age in that study was 35.6 ± 11.7 years, while the mean age in the current study was 72.1 ± 8.1 years. The differences in age and cataract density might have affected the reproducibility of the posterior lens measurements. Neri et al. reported that the ICC of lens thickness measurements was 0.991 using the CASIA SS-1000 [25]. Zeng et al. also reported that the intraobserver and intervisit ICCs for lens thickness measurements ranged from 0.996 to 0.999 using time-domain AS-OCT [13]. In their study, measurement of lens thickness by time-domain AS-OCT failed in 9.1% of eyes. In contrast, we observed no failure of lens measurement by the CASIA2 in the present study, even when patients with advanced cataract were included.

Accurate measurement of crystalline lens geometry, including the lens thickness, is essential for a better understanding of the accommodation mechanism, origin of presbyopia, and sources of optical aberrations, refractive index distribution to

Lens thickness

ACD

Fig. 5 Significant correlations in the lens thickness and aqueous depth (AQD) were observed between the CASIA2 and EAS-1000 (Pearson correlation coefficient, r = 0.682, $P < 0.0001$ and r = 0.972, $P < 0.0001$). The line of equivalence ($y = x$) is shown by the dotted line. The difference in mean lens thickness and aqueous depth (AQD) measurements between the CASIA2 and EAS-1000 is shown. The mean $\pm$ 1.96 standard deviation is also indicated

the optical changes occurring during aging [1, 13–16, 30]. The geometry of the crystalline lens has been reported using different techniques. Purkinje imaging has been used to estimate the radii of curvature of the different ocular components that are estimated from the relative height of images of the light source [31]. However, this Purkinje imaging technique does not provide an image of the anterior chamber of the eye. Scheimpflug imaging provides cross-sectional images of the crystalline lens. However, Scheimpflug imaging, which involves visible light sources, cannot clearly depict the anterior chamber angle and frequently limits the view of the posterior lens. In the current study, the posterior lens could be measured by Scheimpflug imaging in only 6% of patients and by the EAS-1000 in 27%. The inclusion of aged participants and eyes with cataract may have affected these results. Dubbelman et al. reported a positive relationship between age and lens thickness using the EAS-1000 after correction of distortion due to refraction of the cornea and lens [32]. In the current study, we also found that the thickness of the crystalline lens was age-dependent (data not shown), which is consistent with previous reports [33–35]. No previous study has compared lens thickness between a Scheimpflug imaging system and AS-OCT. Previous studies have shown lower or similar ACD measurement values between Scheimpflug imaging and AS-OCT [20, 36].

Nakamura et al. reported a higher value of ACD in Scheimpflug imaging than when using the CASIA SS-1000 [37]. Wang et al. reported that the thickest ACD was obtained with the Galilei dual Scheimpflug camera followed in order by the Placido disk corneal topographer (Ziemer Ophthalmic Systems AG, Port, Switzerland), Visante, time-domain AS-OCT (Carl Zeiss Meditec AG, Jena, Germany), Sirius rotating single Scheimpflug camera combined with a Placido disk corneal topographer (Costruzione Strumenti Oftalmici, Florence, Italy), and Pentacam [38]. In the current study, the AQD measurements by the Pentacam and EAS-1000 were significantly lower than those by the CASIA2.

No statistically significant difference was found in the lens thickness measurements between the CASIA2 and AL-4000. Zeng et al. reported that time-domain AS-OCT tended to give greater lens thickness values than the A-scan ultrasonography [13]. Ultrasonography estimates the distances according to the velocity of sound in ocular media and the ultrasonic echoes from the interfaces of each ocular structure. However, the velocity of sound in the crystalline lens must be known to accurately determine the lens thickness when using ultrasonography. In contrast, OCT quantifies the distance based on a linear scan using infrared light and the principles of low-coherence interferometry. The different physical principles

of these two measurements affected the results of the previous and current studies. Different lens conditions between both studies may have affected the results. In the current study, ACD (CCT + AQD) was significantly higher by the CASIA2 than AL-4000. Other previous studies reported that AS-OCT tends to underestimate or display a similar value for the CCT [20, 39, 40]; however, it overestimates the ACD compared with ultrasonography [41].

The tilting amount was $4.86 \pm 1.52°$ with CASIA2 in the current study. The definition of lens thickness in the current study was along the vertex normal and might be affected by tilt. We measured CCT/AQD/ACD on optical axis with CASIA SS-1000 and CASIA2. On the other hand, CCT/AQD/ACD measurements with ultrasonic pachymetry or Scheimpflug camera is limited to vertex normal and it might be affected by tilt. Previous study reported that a centering error from the eye's geometric center gave an undervaluation for anterior chamber depth [42, 43]. The IOLMaster (Carl Zeiss Meditec, Jena, Germany) measures the anterior chamber depth along the vertex normal, whereas AS-OCT (Visante™, Carl Zeiss Meditec, Dublin, California, USA) measures along the optical axis. The AS-OCT showed higher repeatability than IOLMaster. Being in the optical axis, the AS-OCT measurements probably reflect a more accurate estimation of anterior chamber depth. Kriechbaum K et al. compared the ACD along vertex normal (IOLMaster) and optical axis (PCI laboratory prototype) and there was no significant difference [44].

This study has some limitations. The relatively small sample size may have affected the ability to detect subtle differences in biometric and lens characteristics.

In conclusion, we evaluated the biometric measurements of the anterior eye segment by the CASIA2. The CASIA2 techniques yielded measurements comparable with those of the CASIA SS-1000, A-scan ultrasonography, and Scheimpflug camera. However, the presence of mild cataract decreased the repeatability of measurements of the posterior part of the lens.

Compliance with Ethical Standards

The research protocol was approved by the Tsukuba University Hospital Institutional Review Board, and written informed consent was obtained from each patient. The study adhered to the tenets of Declaration of Helsinki.

References

1. Brown N (1974) The change in lens curvature with age. Exp Eye Res 19:175–183
2. Dubbelman M, Van der Heijde GL (2001) The shape of the aging human lens: curvature, equivalent refractive index and the lens paradox. Vis Res 41:1867–1877
3. Hamzeh N, Moghimi S, Latifi G, Mohammadi M, Khatibi N, Lin SC (2015) Lens thickness assessment: anterior segment optical coherence tomography versus A-scan ultrasonography. Int J Ophthalmol 8:1151–1155
4. Yeter V, Aritürk N, Birinci H, Süllü Y, Güngör İ (2015) Effects of birth weight on anterior segment measurements in full-term children without low birth weight by dual-Scheimpflug analyzer. Am J Ophthalmol 160:832–840.e1
5. Gambra E, Ortiz S, Perez-Merino P, Gora M, Wojtkowski M, Marcos S (2013) Static and dynamic crystalline lens accommodation evaluated using quantitative 3-D OCT. Biomed Opt Express 4:1595–1609
6. Richdale K, Bullimore MA, Zadnik K (2008) Lens thickness with age and accommodation by optical coherence tomography. Ophthalmic Physiol Opt 28:441–447
7. Swarbrick HA, Wong G, O'Leary DJ (1998) Corneal response to orthokeratology. Optom Vis Sci 75:791–799
8. Doughty MJ, Zaman ML (2000) Human corneal thickness and its impact on intraocular pressure measures: a review and meta-analysis approach. Surv Ophthalmol 44:367–408
9. Fukuda S, Beheregaray S, Hoshi S, Yamanari M, Lim Y, Hiraoka T, Yasuno Y, Oshika T (2013) Comparison of three-dimensional optical coherence tomography and combining a rotating Scheimpflug camera with a Placido topography system for forme fruste keratoconus diagnosis. Br J Ophthalmol 97:1554–1559
10. Devereux JG, Foster PJ, Baasanhu J, Uranchimeg D, Lee PS, Erdenbeleig T, Machin D, Johnson GJ, Alsbirk PH (2000) Anterior chamber depth measurement as a screening tool for primary angle-closure glaucoma in an East Asian population. Arch Ophthalmol 118:257–263
11. Langenbucher A, Huber S, Nguyen NX, Seitz B, Gusek-Schneider GC, Küchle M (2003) Measurement of accommodation after implantation of an accommodating posterior chamber intraocular lens. J Cataract Refract Surg 29:677–685
12. Olsen T (2007) Calculation of intraocular lens power: a review. Acta Ophthalmol Scand 85:472–485
13. Zeng Y, Liu Y, Liu X, Chen C, Xia Y, Lu M, He M (2009) Comparison of lens thickness measurements using the anterior segment optical coherence tomography and A-scan ultrasonography. Invest Ophthalmol Vis Sci 50:290–294
14. Mutti DO, Zadnik K, Fusaro RE, Friedman NE, Sholtz RI, Adams AJ (1998) Optical and structural development of the crystalline lens in childhood. Invest Ophthalmol Vis Sci 39:120–133
15. García-Domene MC, Díez-Ajenjo MA, Gracia V, Felipe A, Artigas JM (2011) A simple description of age-related changes in crystalline lens thickness. Eur J Ophthalmol 21:597–603
16. Ishii K, Yamanari M, Iwata H, Yasuno Y, Oshika T (2013) Relationship between changes in crystalline lens shape and axial elongation in young children. Invest Ophthalmol Vis Sci 54:771–777
17. Huang D, Swanson EA, Lin CP, Schuman JS, Stinson WG, Chang W, Hee MR, Flotte T, Gregory K, Puliafito CA, Fujimoto JG (1991) Optical coherence tomography. Science 254:1178–1181

18. Mohamed S, Lee GK, Rao SK, Wong AL, Cheng AC, Li EY, Chi SC, Lam DS (2007) Repeatability and reproducibility of pachymetric mapping with Visante anterior segment-optical coherence tomography. Invest Ophthalmol Vis Sci 48:5499–5504

19. Fukuda S, Kawana K, Yasuno Y, Oshika T (2010) Repeatability and reproducibility of anterior ocular biometric measurements with 2-dimensional and 3-dimensional optical coherence tomography. J Cataract Refract Surg 36:1867–1873

20. Fukuda S, Kawana K, Yasuno Y, Oshika T (2009) Anterior ocular biometry using 3-dimensional optical coherence tomography. Ophthalmology 116:882–889

21. Shoji T, Kato N, Ishikawa S, Ibuki H, Yamada N, Kimura I, Shinoda K (2017) In vivo crystalline lens measurements with novel swept-source optical coherent tomography: an investigation on variability of measurement. BMJ Open Ophthalmol 1:e000058

22. Hoffer KJ (2011) Definition of ACD. Ophthalmology 118:1484

23. Yoo YS, Whang WJ, Hwang KY, Lazo M, Hwang JH, Joo CK, Yoon G (2019) Use of the crystalline lens equatorial plane as a new parameter for predicting postoperative intraocular lens position. Am J Ophthalmol 198:17–24

24. Bland JM, Altman DG (1995) Comparing methods of measurement: why plotting difference against standard method is misleading. Lancet 346:1085–1087

25. Neri A, Ruggeri M, Protti A, Leaci R, Gandolfi SA, Macaluso C (2015) Dynamic imaging of accommodation by swept-source anterior segment optical coherence tomography. J Cataract Refract Surg 41:501–510

26. Zhong J, Tao A, Xu Z, Jiang H, Shao Y, Zhang H, Liu C, Wang J (2014) Whole eye axial biometry during accommodation using ultra-long scan depth optical coherence tomography. Am J Ophthalmol 157:1064–1069

27. Ruggeri M, Uhlhorn SR, De Freitas C, Ho A, Manns F, Parel JM (2012) Imaging and full-length biometry of the eye during accommodation using spectral domain OCT with an optical switch. Biomed Opt Express 3:1506–1520

28. Xu BY, Mai DD, Penteado RC, Saunders L, Weinreb RN (2017) Reproducibility and agreement of anterior segment parameter measurements obtained using the CASIA2 and Spectralis OCT2 optical coherence tomography devices. J Glaucoma 26:974–979

29. Chansangpetch S, Nguyen A, Mora M, Badr M, He M, Porco TC, Lin SC (2018) Agreement of anterior segment parameters obtained from swept-source Fourier-domain and time-domain anterior segment optical coherence tomography. Invest Ophthalmol Vis Sci 59:1554–1561

30. Marcos S, Burns SA, Moreno-Barriusop E, Navarro R (1999) A new approach to the study of ocular chromatic aberrations. Vis Res 39:4309–4323

31. Rosales P, Dubbelman M, Marcos S, van der Heijde R (2006) Crystalline lens radii of curvature from Purkinje and Scheimpflug imaging. J Vis 6:1057–1067

32. Dubbelman M, van der Heijde GL, Weeber HA (2001) The thickness of the aging human lens obtained from corrected Scheimpflug images. Optom Vis Sci 78:411–416

33. Koretz JF, Neider MW, Kaufman PL, Bertasso AM, DeRousseau CJ, Bito LZ (1987) Slit-lamp studies of the rhesus monkey eye. I. Survey of the anterior segment. Exp Eye Res 44:307–318

34. Praveen MR, Vasavada AR, Shah SK, Shah CB, Patel UP, Dixit NV, Rawal S (2009) Lens thickness of Indian eyes: impact of isolated lens opacity, age, axial length, and influence on anterior chamber depth. Eye (Lond) 23:1542–1548

35. Klein BE, Klein R, Moss SE (1998) Correlates of lens thickness: the Beaver Dam Eye Study. Invest Ophthalmol Vis Sci 39:1507–1510

36. Fu J, Wang X, Li S, Wu G, Wang N (2010) Comparative study of anterior segment measurement with Pentacam and anterior segment optical coherence tomography. Can J Ophthalmol 45:627–631

37. Nakakura S, Mori E, Nagatomi N, Tabuchi H, Kiuchi Y (2012) Comparison of anterior chamber depth measurements by 3-dimensional optical coherence tomography, partial coherence interferometry biometry, Scheimpflug rotating camera imaging, and ultrasound biomicroscopy. J Cataract Refract Surg 38:1207–1213

38. Wang Q, Ding X, Savini G, Chen H, Feng Y, Pan C, Hua Y, Huang J (2012) Anterior chamber depth measurements using Scheimpflug imaging and optical coherence tomography: repeatability, reproducibility, and agreement. J Cataract Refract Surg 41:178–185

39. Kim HY, Budenz DL, Lee PS, Feuer WJ, Barton K (2008) Comparison of central corneal thickness using anterior segment optical coherence tomography vs ultrasound pachymetry. Am J Ophthalmol 145:228–232

40. Zhao PS, Wong TY, Wong WL, Saw SM, Aung T (2007) Comparison of central corneal thickness measurements by visante anterior segment optical coherence tomography with ultrasound pachymetry. Am J Ophthalmol 143:1047–1049

41. Nemeth G, Vajas A, Tsorbatzoglou A, Kolozsvari B, Modis L Jr, Berta A (2007) Assessment and reproducibility of anterior chamber depth measurement with anterior segment optical coherence tomography compared with immersion ultrasonography. J Cataract Refract Surg 33:443–447

42. Baikoff G, Jitsuo Jodai H, Bourgeon G (2005) Measurement of the internal diameter and depth of the anterior chamber: IOLMaster versus anterior chamber optical coherence tomographer. J Cataract Refract Surg 31:1722–1728

43. Lavanya R, Teo L, Friedman DS, Aung HT, Baskaran M, Gao H, Alfred T, Seah SK, Kashiwagi K, Foster PJ, Aung T (2007) Comparison of anterior chamber depth measurements using the IOLMaster, scanning peripheral anterior chamber depth analyser, and anterior segment optical coherence tomography. Br J Ophthalmol 91:1023–1026

44. Kriechbaum K, Findl O, Kiss B, Sacu S, Petternel V, Drexler W (2003) Comparison of anterior chamber depth measurement methods in phakic and pseudophakic eyes. J Cataract Refract Surg 29:89–894